
















# The LSST Science Pipelines Software: Optical Survey Pipelined Reduction and Analysis Environment

RUBIN OBSERVATORY SCIENCE PIPELINES DEVELOPERS, JAMES F. BOSCH <sup>2</sup>, YUSRA ALSAYYAD <sup>2</sup>, TIM JENNESS <sup>3</sup>,  
ERIC C. BELLM <sup>4</sup>, ROBERT H. LUPTON <sup>2</sup>, NATE B. LUST <sup>2</sup>, IAN S. SULLIVAN <sup>4</sup>, CHRISTOPHER Z. WATERS <sup>2</sup>,  
KRZYSZTOF FINDEISEN <sup>4</sup>, ERFAN NOURBAKHSH <sup>2</sup>, AGNÈS F. FERTÉ <sup>5</sup>, ARUN KANNAWADI <sup>6,2</sup>, ELI S. RYKOFF <sup>7</sup>,  
ANDRÉS A. PLAZAS MALAGÓN <sup>5,7</sup> AND K. SIMON KRUGHOFF <sup>3,\*</sup>

THE RUBIN OBSERVATORY SCIENCE PIPELINES TEAM

1

<sup>2</sup>*Department of Astrophysical Sciences, Princeton University, Princeton, NJ 08544, USA*

<sup>3</sup>*Vera C. Rubin Observatory Project Office, 950 N. Cherry Ave., Tucson, AZ 85719, USA*

<sup>4</sup>*University of Washington, Dept. of Astronomy, Box 351580, Seattle, WA 98195, USA*

<sup>5</sup>*SLAC National Accelerator Laboratory, 2575 Sand Hill Rd., Menlo Park, CA 94025, USA*

<sup>6</sup>*Department of Physics, Duke University, Durham, NC 27708, USA*

<sup>7</sup>*Kavli Institute for Particle Astrophysics and Cosmology, SLAC National Accelerator Laboratory, 2575 Sand Hill Rd., Menlo Park, CA 94025, USA*

## ABSTRACT

The NSF-DOE Vera C. Rubin Observatory will produce the Legacy Survey of Space and Time (LSST) and produce 11 data releases over the ten-year survey. The LSST Science Pipelines Software will be used to create these data releases and to perform the nightly alert production. This paper provides an overview of the LSST Science Pipelines Software and describes the components and how they are combined to form pipelines.

*Keywords:* Astrophysics - Instrumentation and Methods for Astrophysics — methods: data analysis — methods: miscellaneous

## 1. INTRODUCTION

The NSF-DOE Vera C. Rubin Observatory will be performing the 10-year Legacy Survey of Space and Time (LSST; [Ž. Ivezić et al. 2019](#)) starting in 2025. Rubin Observatory is located on Cerro Pachon in Chile and consists of the 8.4m Simonyi Survey Telescope ([S. J. Thomas et al. 2022](#)) with the 3.2-gigapixel LSSTCam survey camera ([A. Roodman et al. 2024](#)) performing the main survey and the Rubin Auxiliary Telescope ([P. Ingraham et al. 2020](#)) providing supplementary atmospheric calibration data. The Data Management System (DMS; [W. O’Mullane et al. 2022](#)) is designed to handle the flow of data from the telescope, approaching 20 TB per night, in order to issue alerts and to prepare annual data releases. A central component of the DMS is the LSST Science Pipelines software that provides the algorithms and frameworks required to process the data from the LSST and generate the coadds, difference im-

ages, and catalogs to the user community for scientific analysis.

The LSST Science Pipelines software consists of the building blocks and pipeline infrastructure required to construct high performance pipelines to process the data from LSST. It has been under development since at least 2004 ([T. Axelrod et al. 2004](#)) and has evolved significantly over the years as the project transitioned from prototyping ([T. Axelrod et al. 2010](#)) and entered into formal construction ([M. Jurić et al. 2017](#)). The software is designed to be usable by other optical telescopes and this has been demonstrated with Hyper Suprime Cam on the Subaru Telescope in Hawaii ([J. Bosch et al. 2018](#)) and also with data from the Dark Energy Camera (DECam), the VISTA infrared camera (VIRCAM), the Wide Field Survey Telescope (WFST; [M. Cai et al. 2025](#)), and the Gravitational-wave Optical Transient Observer (GOTO; [J. R. Mullaney et al. 2021](#)).

In this paper we provide an overview of the components of the software system. This includes a description of the support libraries and data access abstraction, the

\* Author is deceased

pipeline task system, and an overview of the algorithmic components. We do not include details of the science validation of the individual algorithms. The other components of the LSST DMS, such as the workflow system (M. Gower et al. 2022; E. Karavakis et al. 2024), the Qserv database (D. L. Wang et al. 2011; F. Mueller et al. 2023) and the Rubin Science Platform (M. Jurić et al. 2019; W. O’Mullane et al. 2024), are not covered in this paper.

## 2. FUNDAMENTALS

The LSST Science Pipelines software is written in Python with C++ used for high-performance algorithms and for core classes that are usable in both languages. We use Python 3 (having ported from python 2, T. Jenness 2020, currently with a minimum version of Python 3.12), and the C++ layer can use C++17 features with pybind11 being used to provide the interface from Python to C++. Additionally, the C++ layer uses `ndarray` to allow seamless passing of C++ arrays to and from Python `numpy` arrays. This compatibility with `numpy` is important in that it makes LSST data structures available to standard Python libraries such as Scipy and Astropy (T. Jenness et al. 2016; Astropy Collaboration et al. 2018).

Although all the software uses the `lsst` namespace, the code base is split into individual Python products in the LSST GitHub organization<sup>8</sup> that can be installed independently and which declare their own dependencies. These dependencies are managed using the “Extended Unix Product System” (EUPS; N. Padmanabhan et al. 2015; T. Jenness et al. 2018) where most of the products are built using the SCons system (S. Knight 2005) with LSST-specific extensions provided in the `sconsUtils` package enforcing standard build rules and creating the necessary Python package metadata files.

For logging we always use standard Python logging with an additional `VERBOSE` log level between `INFO` and `DEBUG` to provide additional non-debugging detail that can be enabled during batch processing. This verbose logging is used for periodic logging where long-lived analysis tasks are required to issue a log message every 10 minutes to indicate to the batch system that they are still alive and actively performing work. For logging from C++ we use `Log4CXX` wrapped in the `lsst.log` package to make it look more like standard Python logging, whilst also supporting deferred string formatting such that log messages are only formed if the log message level is sufficient for the message to be logged. These C++ log messages are forwarded to

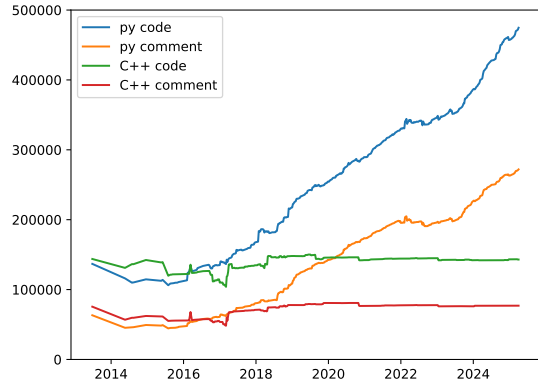


**Figure 1.** The number of lines of code comprising the LSST Science Pipelines software as a function of year. Line counts include comments but not blank lines. Python interfaces are implemented using `pybind11` and that is counted as C++ code. For the purposes of this count Science pipelines software is defined as the `lsst_distrib` metapackage and does not include code from third party packages.

Python rather than being issued from an independent logging stream. Finally, we also provide some LSST-specific exceptions that can be thrown from C++ code and caught in Python.

As of April 2025, the Science Pipelines software is approximately 700,000 lines of Python and 225,000 lines of C++. The number of lines in the pipelines code as a function of time is given in Fig. 1.

### 2.1. Python environment

An important aspect of running a large data processing campaign is to ensure that the software environment is well defined. We define a base python environment using conda-forge via a meta package named `rubin-env`<sup>9</sup>. This specifies all the software needed to build and run the science pipelines software. A Docker container is built for each software release and the fully-specified versions of all software are recorded to ensure repeatability.

### 2.2. Unit Testing and Code Coverage

Unit testing and code coverage are critical components of code quality (T. Jenness et al. 2018). Every package comes with unit tests written using the standard `unittest` module. We run the tests using `pytest` (H. Krekel 2017) and this comes with many advantages in that all the tests run in the same process and requiring global parameters to be well understood, tests can be run in parallel in multiple processes, plugins can be enabled to extend testing and record test coverage, and a test report can be created giving details of run times

<sup>8</sup> <https://github.com/lsst>

<sup>9</sup> <https://github.com/conda-forge/rubinenvironment-feedstock>

**Table 1.** Common dimensions present in the default dimension universe.

Name	Description
<code>instrument</code>	Instrument.
<code>band</code>	Waveband of interest.
<code>physical_filter</code>	Filter used for the exposure.
<code>day_obs</code>	The observing day.
<code>group</code>	Group identifier.
<code>exposure</code>	Individual exposure.
<code>visit</code>	Collection of 1 or 2 exposures.
<code>tract</code>	Tesselation of the sky.
<code>patch</code>	Patch within a tract.

and test failures. Coding standards compliance with PEP 8 (G. van Rossum 2013) is enforced using GitHub Actions, the `ruff` package, and `pre-commit` checks. A Jenkins system provides the team with continuous integration facilities that includes running longer tests with pre-cursor datasets.

### 3. DATA ACCESS ABSTRACTION

#### 3.1. Butler

Early in the development of the LSST Science Pipelines software it was decided that the algorithmic code should be written without knowing where files came from, what format they were written in, where the outputs are going to be written or how they are going to be stored. All that the algorithmic code needs to know is the relevant data model and the Python type. To meet these requirements we developed a library called the Data Butler (see e.g., T. Jenness et al. 2022; N. B. Lust et al. 2023).

The Butler internally is implemented as a registry, a database keeping track of datasets, and a datastore, a storage system that can map a Butler dataset to a specific collection of bytes. A datastore is usually a file store (including POSIX file system, S3 object stores, or WebDAV) but it is also possible to store metrics directly into the Sasquatch metrics service (A. Fausti 2023; A. Fausti Neto et al. 2024).

A core concept of the Butler is that every dataset must be given what we call a “data coordinate.” The data coordinate locates the dataset in the dimensional space where dimensions are defined in terms that scientists understand. Some commonly used dimensions are listed in Table 1. Each dataset is uniquely located by specifying its dataset type, its run collection, and its co-

ordinates, with Butler refusing to accept another dataset that matches all three of those values. The dataset type defines the relevant dimensions (such as whether this is referring to observations or a sky map) and the associated Python type representing the dataset. The run collection can be thought of as a folder grouping datasets created by the same batch operation, but does not have to be a folder within a file system.

As a concrete example, the file from one detector of an LSSTCam observation taken sometime in 2025 could have a data coordinate of `instrument="LSSTCam", detector=42, exposure=2025080300100` and be associated with a `raw` dataset type. The `exposure` record itself implies other information such as the physical filter and the time of observation. A deep coadd on a patch of sky would not have `exposure` dimensions at all and would instead be something like `instrument="LSSTCam", tract=105, patch=2, skymap="something"`, which would tell you exactly where it is located in the sky since you can calculate it from the tract and patch and skymap.

#### 3.2. Instrument Abstractions: Obs Packages

The Butler and pipeline construction code know nothing about the specifics of a particular instrument. In the default dimension universe there is an `instrument` dimension that includes a field containing the full name of a Python `Instrument` class. This class, which uses a standard interface, is used by the system to isolate the instrument-specific from the pipeline-generic. Some of the responsibilities are:

- Register instrument-specific dimensions such as `detector`, `physical_filter` and the default `visit_system`.
- Define the default `raw` dataset type and the associated dimensions.
- Provide configuration defaults for pipeline task code that is processing data from this instrument.
- Provide a “formatter” class that knows how to read raw data.
- Define the default curated calibrations known to this instrument.

By convention we define the instrument class and associated configuration in `obs` packages. As an extension to the base definition of an “instrument”, the LSST Science Pipelines define a modified `Instrument` class that includes focal plane distortions using the `afw` package (see §4.3). There are currently project-supported `obs` packages for:

- LSSTCam (A. Roodman et al. 2024; T. Lange et al. 2024; Y. Utsumi et al. 2024; S. M. Kahn et al. 2010), LATISS (P. Ingraham et al. 2020), and associated Rubin Observatory test stands and simulators.
- Hyper-SuprimeCam (S. Miyazaki et al. 2018).
- The Dark Energy Camera (B. Flaugher et al. 2015; D. L. DePoy et al. 2008).
- CFHT’s MegaPrime (O. Boulade et al. 2003).

Additionally, teams outside the project have developed `obs` packages to support Subaru’s Prime Focus Spectrograph (S.-Y. Wang et al. 2020), VISTA’s VIR-CAM (W. Sutherland et al. 2015), the Wide Field Survey Telescope (WFST; M. Cai et al. 2025), and the Gravitational-wave Optical Transient Observer (GOTO; J. R. Mullaney et al. 2021).

### 3.3. Metadata Translation

Every instrument uses different metadata standards but the Butler data model and pipelines require some form of standardization to determine values such as the coordinates of an observation, the observation type, or the time of observation. To perform that standard extraction of metadata each supported instrument must provide a metadata translator class using the `astro_metadata_translator` infrastructure.<sup>10</sup> The translator classes can understand evolving data models and allow the standardized metadata to be extracted for the lifetime of an instrument even if headers changed. Furthermore, in addition to providing standardized metadata the package can also provide programmatic or per-exposure corrections to data headers prior to calculating the translated metadata. This allows files that were written with incorrect headers to be recovered during file ingestion.

## 4. CORE INFRASTRUCTURE LIBRARIES

### 4.1. Region Handling

The `sphgeom` package is used for spherical geometry calculations, sky-based region definitions, and sky pixelization schemes. The `geom` package is used to locations and extents within a Cartesian coordinate space.

(Aside: I only just realized that `lsst.geom` has `SpherePoint` that is effectively `LonLat` from `sphgeom` and we have both `lsst.geom.Angle` and `lsst.sphgeom.Angle`... I feel like if I document this, that questions will be asked...)

For coordinates, we use ICRS everywhere and leave any required coordinate transformations to the Astropy infrastructure.

### 4.2. Time and Hierarchical Data Structures

The `daf_base` package provides core data structures for handling time and hierarchical data structures. The `DateTime` package is used in our C++ data models mostly to represent TAI times. For general manipulations of times in Python we now use `astropy.time`, following the recommendations from T. Jenness et al. (2016).

The `PropertySet` and `PropertyList` classes allow dict-like data structures to be passed from Python to C++ and back again. The `PropertySet` represents a hierarchical key/value data structure whereas `PropertyList` is a flat data structure that is used to represent a FITS header and supports multi-valued keys and key comments.

### 4.3. Application Framework

`afw` – this is called the “Application Framework” in T. Axelrod et al. (2010)<sup>11</sup>

- Image/MaskedImage/Exposure
- Table and Catalogs.
- Detection
- Math
- Camera geometry
- FITS I/O
- WCS: AST library (D. S. Berry et al. 2016) backs the world coordinate system handling.

### 4.4. Co-add Utilities

`coadd_utils` ?

## 5. INSTRUMENT SIGNATURE REMOVAL

Raw images from charge-coupled devices (CCDs) contain instrumental effects, such as dark currents, clocking artifacts, or crosstalk between neighboring amplifiers, that can be removed in the data processing. In the Rubin pipeline, this step is called Instrument Signature Removal (ISR) and is the first processing applied to a raw CCD exposure. The package performing the ISR on an exposure, called `ip_isr`, is detailed below in Sec.

<sup>10</sup> <https://astro-metadata-translator.lsst.io>

<sup>11</sup> This document can be downloaded from <https://lsst/Document-9349>



5.1: it is a critical package for Data Release Pipeline (DRP) used to process LSST images and requires calibration products produced and verified by `cp_pipe` and `cp_verify` respectively as described in Sec. 11.3.1. For further information about the life cycle of a calibration product and the procedures it entails, see C. Waters (2025). In Sec. 5.2, we specifically describe the correction of amplifier offset in more detail. A general overview of the ISR steps (based on the model in Fig. 2) and calibration products production (including generation, verification, certification, approval, and distribution) is given in A. A. Plazas Malagón et al. (2024).

We note that we focus here on our approach to performing ISR on data from LSST cameras only (LSST-Cam, ComCam, and LATISS), although we also provide calibration pipelines for other cameras such as DECam and HSC (using a different ISR approach).

### 5.1. ISR package

Exposures from LSST cameras are affected by instrumental effects, ranging from well-known CCD effects like dark currents or bias levels to effects more recently characterized like tree-rings (see H. Y. Park et al. (2017); H. Park et al. (2020); J. H. Esteves et al. (2023); Y. Okura et al. (2015, 2016) for more details on tree rings in LSSTCam and their impact on science) or the Brighter-Fatter effect as discussed in A. Broughton et al. (2024). Correcting for these effects requires specific calibrations, which we refer to as calibration products. In LSST cameras, calibration products typically are a combined bias, a combined dark, a Photon Transfer Curve (PTC), a crosstalk matrix, a list of defects, and a look-up table of non-linearity parameters. The meaning of these calibration products and the details on the Rubin Observatory’s ISR and calibration approach can be found in A. A. Plazas Malagón et al. (2024) and (P. Fagrelus & E. Rykoff 2025).

The `ip_isr` package<sup>12</sup> contains the codes needed to remove instrument signatures in exposures from LSST cameras and to produce calibration products. To inform our ISR approach, we first designed a model of the instrument, displayed in Fig. 2, based on our knowledge of the hardware and electronics. This model states the order in which the different known instrumental effects happen, from a photon hitting the CCD to the output ADC unit (ADU) signal. In turn, `isrTaskLSST` in `ip_isr` sequentially applies corrections of these effects in the opposite order as their effects occur in the model, as we are attempting to remove the impact of those effects on the image. Such corrections are typically done

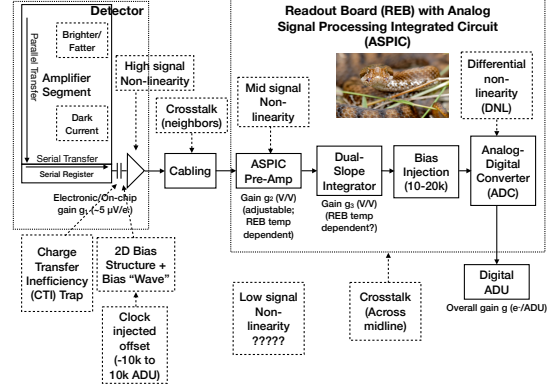


**Figure 2.** Schematic of the instrument model for detector effects in LSST cameras which `isrTaskLSST` is based on at the time of publication. More details about the model can be found in P. Fagrelus & E. Rykoff (2025) and A. A. Plazas Malagón et al. (2024).

by calling other `Tasks` (e.g. overscan, crosstalk, etc.) also implemented in `ip_isr`.

Overall, `isrTaskLSST` takes a raw CCD exposure, and calibration products if available, and outputs a `Struct` containing the output exposure, the `postISRCDD` output exposure as well as its binned version for easier display, the exposure without interpolation and statistics on the output exposure. `IsrTaskLSSTConfig` defines the configurations used in this `Task`, they are set by default to their expected value to perform ISR on a typical LSSTCam exposure. Configuration parameters starting with `do` will typically correspond to an ISR step, they are turned on or off in the pipelines when producing the different calibration products. We have also developed `isrMockLSST` which simulates a raw exposure and corresponding calibration products and is used to test `isrTaskLSST`.

### 5.2. Amplifier Offset Correction

The amplifier offset correction (commonly referred to as amp-offset correction, or pattern continuity correction) runs as part of the instrument signature removal (ISR) process. This correction is designed to address systematic discontinuities in background sky levels across amplifier boundaries. We believe that these discontinuities arise from electronic biases between adjacent amplifiers, persisting even after the application of dark and flat corrections.

Drawing on the PANSTARRS’ Pattern Continuity algorithm (C. Z. Waters et al. 2020), our method aims to eliminate these offsets, thereby preventing problems such as background over-/under-subtraction at amplifier boundaries caused by discontinuities across the detector.

<sup>12</sup> [https://github.com/lsst/ip\\_isr](https://github.com/lsst/ip_isr)

The amp-offset algorithm initially computes a robust flux difference measure between two narrow strips on opposite sides of each amplifier-amplifier interface. Regions containing detected sources, or pixel data which have been masked for other reasons, are not considered. These amp-interface differences are stored in an amp-offset matrix; diagonal entries represent the number of neighboring amplifiers, and off-diagonal entries encode information about the associations between amplifiers. A complementary interface matrix encodes directional information for these associations. Using this information, a least-squares minimization is performed to determine the optimal pedestal value to be added or subtracted to each amp which would reduce the amp-offset between that amplifier and all of its neighboring amplifiers. This method is generalized to support 2D amplifier geometries within a detector, as with LSSTCam, incorporating length-based weighting into the matrices to account for amplifiers that are not square.

## 6. MEASUREMENT SYSTEM

Measurement plugin system.

`meas_base`

### 6.1. *meas\_algorithms*

### 6.2. *meas\_deblender*

### 6.3. *meas\_extensions\_convolved*

### 6.4. *meas\_extensions\_gaap*

`meas_extensions_gaap` implements the Gaussian Aperture and PSF photometry (GAaP) algorithm (K. Kuijken 2008). It is an aperture photometry algorithm designed to obtain consistent colors of extended objects (i.e., galaxies). This is done by weighting each (pre-seeing) region of a galaxy by the same pre-defined 2D Gaussian function in all the bands and is thus largely insensitive to the seeing conditions in the different bands. In practice, this is done by first convolving each object by a kernel (using the same tools described in Sec. 7) so that the PSF is Gaussian and is larger by about 15% (this is configurable). As a second step, each Gaussianized object is then weighted with a Gaussian aperture so that the effective pre-seeing Gaussian aperture is the same for all objects in all the bands. The plugin is configured to use a series of circular Gaussian apertures, an elliptical Gaussian aperture (optionally) that matches the shape of the object in the reference band.

Although the two-step approach is motivated by the original implementation in K. Kuijken (2008), the implementation of this algorithm within the broader context of the measurement framework makes it different from the implementation used in the Kilo-Degree Survey (KiDS; A. H. Wright et al. 2025). In particular, because

neighboring objects are replaced with noise before measurement, Gaussianization of the PSF does not result in increased blending as mentioned in Appendix A2 of K. Kuijken et al. (2015). Furthermore, the uncertainty handling is different. Correlations in noise introduced due to PSF-Gaussianization is included in the uncertainty estimates. However, because only per-pixel noise variance is tracked, the noise treatment is forced to assume that the noise is uncorrelated to begin with which is not true on the coadds. See A. Kannawadi (2022) for more details on the implementation details.

Note that this measurements from this plugin do not produce total fluxes, but should only be used to obtain colors. For total fluxes, measurements from `cModel` or `MultiProFit` (c.f. Sec. 6.12) are recommended.

### 6.5. *meas\_extensions\_photometryKron*

### 6.6. *PSF Modeling*

Within the pipeline, three distinct PSF models are defined: `pcaPsf`, `PSFex`, and `Piff`. Only `PSFex` and `Piff` are currently used. `PSFex` is a fast, and less accurate PSF estimation and is wrapped within `meas_extensions_psfex`. In contrast, `Piff` is a slightly slower, but more accurate PSF estimation that is incorporated in `meas_extensions_piff`. Both `meas_extensions_psfex` and `meas_extensions_piff` are described below.

#### 6.6.1. *meas\_extensions\_psfex*

#### 6.6.2. *meas\_extensions\_piff*

The `meas_extensions_piff` package is a wrapper around the PSF package `Piff` used to estimate and compute the PSF (M. Jarvis et al. 2021a,b). `Piff` is a modular package that supports various PSF models, interpolation schemes, coordinate systems, and can operate on a per-CCD basis or over the full field of view, as indicated by its name. The implementation within `meas_extensions_piff` does not exploit the full modularity of `Piff`; instead, it closely follows the method used for cosmic shear analysis like in DES (M. Jarvis et al. 2021b; T. Schutt et al. 2025).

The PSF model utilized is a `PixelGrid`, and the interpolation is performed using `BasisPolynomial` interpolation (M. Jarvis et al. 2021b). Modeling is executed per CCD and can employ either pixel or sky coordinates. A key difference from `PSFex` is that `Piff` implements outlier rejection based on chi-squared criteria (see M. Jarvis et al. 2021b, for more details).

Most of the configuration described here is adjustable through the `PiffPsfDeterminerConfig` that are exposing some of the configurable parameters of `Piff` and can be fine-tuned for a dedicated survey. However, some

important features that were implemented by [M. Jarvis et al. \(2021b\)](#) and [T. Schutt et al. \(2025\)](#) have not yet been enabled but will be available in the near future. While [M. Jarvis et al. \(2021b\)](#) operates in sky coordinates with a WCS that includes CCD distortions such as treerings, `meas_extensions_piff` can work in sky coordinates and incorporate WCS; as written, it does not, however, account for CCD distortions like tree rings. Additionally, although [T. Schutt et al. \(2025\)](#) incorporated a color correction to account for chromatic effects on the PSF, this correction has not yet been implemented in `meas_extensions_piff`.

#### 6.7. `meas_extensions_scarlet`

#### 6.8. `meas_extensions_shapeHSM`

The `meas_extensions_shapeHSM` package contains the plugins to measure the shapes of objects. The plugins measure the moments of the sources and PSFs with adaptive Gaussian weights. The algorithm was initially described in [C. Hirata & U. Seljak \(2003\)](#) and was modified later in [R. Mandelbaum et al. \(2005\)](#). The implementation of these algorithms lives within the `hsm` module of the GalSim package ([B. T. P. Rowe et al. 2015](#)). `meas_extensions_shapeHSM` now interacts directly with the Python layer of GalSim to make the measurements.

The base plugin for measuring moments is the `HsmMomentsPlugin` and is the parent class of the `HsmSourceMomentsPlugin` and `HsmPsfMomentsPlugin` which are specialized to measure on the sources (and objects) and PSFs respectively. `HsmSourceMomentsRoundPlugin` is a further specialized plugin that measures the moments with circular Gaussian weights instead of the elliptical ones in `HsmSourceMomentsPlugin`. The `HsmPsfMomentsDebiasedPlugin` adds noise to the PSF image to degrade it to have the same signal-to-noise ratio (SNR) as the source image. This makes the ellipticity calculated from this plugin have the same bias as the source ellipticity. The PSF moments from this plugin should be used when calculating ellipticity residuals so the bias is largely cancelled. Having the various specializations as distinct plugins allows an object to be measured under different configurations simultaneously and included in the output catalogs.

In addition to the plugins that measure (adaptive) weighted moments, there are also a series of `HsmShape` plugins to estimate the PSF-corrected ellipticities of objects. In particular, the outputs from `HsmShapeRegaussPlugin` have been used to measure weak gravitation lensing signals in the Hyper Suprime-

Cam SSP data ([R. Mandelbaum et al. 2018](#); [X. Li et al. 2022](#)).

#### 6.9. `meas_extensions_simpleShape`

#### 6.10. `meas_extensions_trailedSources`

#### 6.11. `meas_modelfit`

#### 6.12. `meas_extensions_multiprofit`

MultiProFit is a package for Gaussian mixture model fitting (?). MultiProFit is primarily used to provide multiband Sersic model fits to objects using all available coadds. The `multiprofit` package is a standalone Python-only package that provides the interfaces for astronomical object fitting. `multiprofit` depends primarily on `gauss2d_fit`, a standalone C++ package with Python bindings for fast evaluation of Gaussian mixture model likelihoods and gradients thereof. `gauss2d_fit` in turn is an extension of `gauss2d`, providing additional classes for parameters with arbitrary limits and transformations from the `modelfit_parameters` header-only C++ library. All of these packages are included in the science pipelines but can also be installed independently, as `multiprofit` only depends on other standalone packages like `pex_config`.

The `meas_extensions_multiprofit` package contains pipeline tasks (with interfaces defined in `pipe_tasks`) necessary to run `multiprofit` on coadded and deblended images. The first of these tasks fits a Gaussian mixture model to the PSF model image at the location of each object in a patch. This procedure is similar to the shapelet PSF fitting functionality in `meas_modelfit`. The main differences are that the components are pure Gaussians (shapelet parameters are not supported), can have independent shapes, and are constrained to have integrals summing to unity (i.e. they are normalized). Currently, only a maximum of two components are supported; this limitation may be removed in the future.

The remainder of the tasks in `meas_extensions_multiprofit` use the Gaussian mixture PSF model to fit a PSF-convolved model to all objects in a given patch, for all available bands. Convenient tasks are available for a variety of models, including a single Sersic, as well as multi-component bulge-disk models with an optional central point source component. In all cases, the structural parameters for each component are band-independent, with a separate total flux parameter for each band. That is, individual components do not have intrinsic color gradients (although the convolved models might, if the PSF parameters vary by band).

### 6.13. Reliability Scoring

The `meas_transiNet` package determines a numerical score for input cutout images using pre-trained machine-learning models. Image differencing may produce false detections, so time-domain surveys characteristically use machine learning classifiers to distinguish astrophysical sources from artifacts (“Real/Bogus;” e.g., [J. S. Bloom et al. 2012](#); [D. A. Goldstein et al. 2015](#); [D. A. Duev et al. 2019](#)).

The `meas_transiNet` defines “model packages” that consist of a python architecture class, a PyTorch ([A. Paszke et al. 2019](#)) weights file, and associated metadata. The inference task may be configured to load a model package from disk or from the Butler.

The `RBTransiNetTask` PipelineTask takes as input three square cutouts of configurable size from the science, template, and difference images centered on the location of a source. These images are concatenated, batched into Torch blobs, and passed to the model for inference. Either CPU or GPU backends may be used for inference. The output of the task is a single float ranging from 0–1 for each cutout triplet, with higher values indicating that the `DIA`Source is more likely to be astrophysical. These reliability scores are then joined with the `DIA`Source catalogs by a later transformation task. Detailed discussion of the model architecture, training, and performance will be presented in T. Acero Cuellar et. al (in prep.).

## 7. DIFFERENCE IMAGING

Difference imaging is implemented in `ip_diffim`, and is divided into three steps. First, a base template image is constructed with `getTemplate` by warping previously-generated coadded images to the WCS and bounding box of the science image. Then the warped template is subtracted from the science image using one of several available algorithms in `subtractImages`, which produces a temporary difference image. Finally, peaks are detected on the difference image and `DIA`Sources are measured in `detectAndMeasure`. The final difference image with updated mask planes is written along with the `DIA`Source catalog.

### 7.1. subtractImages

The primary implementation of image subtraction used by `subtractImages` is based on [C. Alard & R. H. Lupton \(1998\)](#), and uses spatially-varying Gaussian basis functions for the fit. The PSF-matching kernel can be constructed for either the science or the template image, and the resulting difference image is decorrelated [D. J. Reiss & R. H. Lupton \(2016\)](#). Optionally, the science image can be preconvolved with its own PSF before

PSF-matching, producing a Score image analogous to [B. Zackay et al. \(2016\)](#).

### 7.2. detectAndMeasure

Positive and negative peaks are detected by thresholding the Score image if it is available. Otherwise, the difference image is smoothed with a Gaussian of the same width as the PSF of the science image, and thresholds are taken on the smoothed image. Contiguous pixels around each peak that are statistically brighter than the background are grouped into source footprints, and any overlapping footprints are merged. Footprints that contain both a positive and a negative peak are fit as dipoles. The dipole fit simultaneously solves for the negative and positive lobe centroids and fluxes using non-linear least squares minimization. `DIA`Sources that are not classified as dipoles instead fall back on an SDSS-style centroid ([J. R. Pier et al. 2003](#)). Finally, all configured measurement plugins are run, including HSM shape measurements ([C. Hirata & U. Seljak 2003](#); [R. Mandelbaum et al. 2005](#)) and trailed source measurements.

## 8. ASTROMETRIC AND PHOTOMETRIC CALIBRATION

### 8.1. Astrometric Calibration

`meas_astrom gbdes` ([G. M. Bernstein 2022](#); [G. M. Bernstein et al. 2017](#))

Jointcal no longer discussed.

### 8.2. Photometric Calibration

#### 8.3. fgcmcal

Global photometric calibration is computed by use of the Forward Global Calibration Method (FGCM [D. L. Burke et al. 2018](#)), as adopted for LSST Science Pipelines ([P. Fagrelus & E. Rykoff 2025](#)). This global calibration algorithm makes use of repeated observations of stars in all *ugrizy* bands, combining a forward model of the atmospheric parameters with instrumental throughputs measured with auxiliary information. In this way we simultaneously constrain the atmospheric model as well as standardized top-of-atmosphere (TOA) star fluxes over a wide range of star colors, including full chromatic corrections from the instrument and atmosphere.

Running `fgcmcal` first requires generating a look-up table. The input to the look-up table includes the effect of a MODTRAN ([A. Berk et al. 1999](#)) atmospheric model at the elevation of the observatory, as well as the throughput as a function of wavelength and position from the optics, filters, and detector quantum efficiency. The quality of the output (in terms of repeatability of



bright isolated stars across a wide range of colors) depends on the knowledge of the instrumental throughput.

The primary goal of `fgmcal` is to provide a uniform relative photometric calibration of the survey. For “absolute” (relative) calibration, a reference catalog can be used as an additional constraint on the fit. Thus, the overall throughput output by `fgmcal` depends on the reference catalog. This can be checked with (e.g.) specific white dwarfs or CALSPEC (R. C. Bohlin 2007) stars in the survey. However, the relative spatial and chromatic calibration of the `fgmcal` calibration means that the absolute calibration reduces to a set of 6 numbers (one for each band, or one overall throughput and 5 absolute colors).

## 9. SOURCE ASSOCIATION

The `ap_association` package contains multiple tasks for standardizing newly detected `DiaSources` and associating them with existing or new `DiaObjects`. Standardization converts the output catalogs from 7 to the format specified in `sdm_schemas` (Sec. 12), and applies filtering consistent with (W. O’Mullane et al. 2024). Once `DiaSource` catalogs are standardized, they are associated to `DiaObjects` in either of two modes: Data Release Production (DRP) or Alert Production (AP). Both implementations use the Pessimistic Pattern Matcher B (C. B. Morrison 2018) to score and match `DiaSources`, but differ in how `DiaObjects` are stored and how visits are ordered.

- DRP association loads all `DiaSource` catalogs from a set time period overlapping a single patch at once, and creates new `DiaObjects` for matched `DiaSources` from all visits simultaneously.
- AP association processes a single visit at a time, and creates new `DiaObjects` incrementally from unassociated `DiaSources`. `DiaObjects` and their associated `DiaSources` are stored in the Alert Production Database (APDB) (Sec. 9.2).

After association, an additional filtering step may be applied to `DiaSources` with no matched `DiaObject` of Solar System object (Sec 9.1). Properties of the source such as its reliability score (Sec. 6.13, source flags, or signal-to-noise cuts may be used to drop detections that are likely to be false detections and avoid creating erroneous new `DiaObjects`.

### 9.1. Solar System object association

Ephemerides from known Solar System objects are preloaded with approximate locations for the expected time of observation in `mpSkyEphemerisQuery`. Since

these are loaded in Prompt Processing before the science image arrives and is calibrated, the orbital fit parameters are used in association to correct the position to the midpoint of the observation, including the shutter motion profile since the shutter takes a second to cross the focal plane. Solar System objects are associated to `DiaSources` using the closest match within a configurable radius.

### 9.2. Alert Production Database (APDB)

The Alert Production Database (APDB; A. Salnikov & J. McCormick 2024)) supports SQL, Postgres, and Cassandra database formats. The previous history of `DiaObjects`, `DiaSources`, and `DiaForcedSources` for the region containing the science image is loaded with `loadDiaCatalogs`, which are passed to `diaPipe` for association. Loading is split from the association step to enable preloading of catalogs from the database in Prompt Processing during the interval when the next visit has been scheduled but the images have not yet been taken. When AP-style association is run outside of Prompt Processing, it is therefore essential to process all association tasks in strict visit order to prevent loading catalogs from the APDB prematurely and losing `DiaObject` history in association.

## 10. ALERT GENERATION

In order to to enable real-time science, the AP pipelines generate alert packets for each detected `DIASource`. These packets are serialized in Apache Avro<sup>13</sup> format and then transmitted to community alert brokers via Kafka for further processing. M. Patterson et al. (2020) provides a high-level overview of the alert system.

Within the pipelines, alert packets are constructed by `packageAlertsTask` within `ap_association`. Alert packets contain the triggering `DIASource` record; the associated `DIAObject` or `SObject` record; up to twelve months of past history from `DIASources`, `DIAForcedSources`, and/or upper limits; and cutout images of the science, template, and difference images centered at the position of the cutout. Cutouts are provided as FITS images serialized by the astropy `CCDDData` class, and include image, variance, and mask planes along with WCS information and an image of the approximate PSF.

Avro schemas are stored in the `alert_packet` package. They are derived from the corresponding AP schemas in `sdm_schemas` used to instantiate the AP databases.

<sup>13</sup> <https://avro.apache.org/>



## 11. PIPELINES

### 11.1. Pipeline Support

The `Task` Python class provides a standard interface for how to execute an algorithm. The `PipelineTask` variant provides stronger guarantees on configuration and provides a means by which the pipeline execution framework can determine how to link a task into a pipeline and how to determine what type of data should be read from a Butler and what should be written out to a Butler.

Describe `pex_config` because it's not described anywhere.

Pipeline in YAML.

Show plot of a simple pipeline visualization.

Graph building.

Show plot of a graph where a pipeline now includes specific datasets as inputs.

Describe that provenance is stored in the output files and in the graph itself.

Execution system and how BPS provides the interface between a quantum graph and a workflow system.

### 11.2. Task library

#### 11.2.1. `pipe_tasks`

#### 11.2.2. `drp_tasks`

### 11.3. Pipeline Collections

#### 11.3.1. Calibration pipelines

The pipelines to build calibration products (`cp`) for the LSST cameras are defined in `cp_pipe`<sup>14</sup>. They set `isrTaskLSST` configuration parameters needed for each calibration product, by enabling all the sequential steps of the ISR task up to the step before the correction being generated. In some cases, configurations also specify whether to combine exposures (for bias or dark exposures for instance) and to bin exposures to support display.

Once calibration products are produced, they are “verified” (see C. Waters (2025) for more details) using `cp_verify`<sup>15</sup> pipelines by checking they pass metrics defined in R. Lupton et al. (2025). In this case, verify configuration parameters enable all corrections in the ISR task up to and including the application of the correction being verified. As a result, the calibration products can then be certified to be available in the `butler` and used to ISR an exposure.

<sup>14</sup> [https://github.com/lsst/cp\\_pipe](https://github.com/lsst/cp_pipe) and see documentation at <https://pipelines.lsst.io/modules/lsst.cp.pipe/constructing-calibrations.html>

<sup>15</sup> [https://github.com/lsst/cp\\_verify](https://github.com/lsst/cp_verify)

### 11.3.2. `drp_pipe`

#### 11.3.3. `ap_pipe`

The `ap_pipe` package defines the pipeline(s) to be used for real-time Alert Production processing (K.-T. Lim 2022). These pipelines include instrument signature removal (§5), calibration (§??), measurement plugins (§6), image differencing (§7), source association (§9), and alert generation (§10). Some of these tasks are shared with the pipelines in `drp_pipe`, but configured to prioritize speed over strict quality; for example, they use a minimal set of measurement plugins.

`ap_pipe` currently has pipeline variants for LSSTCam, LSSTComCam, LATISS, the Rubin Observatory simulators, Hyper-SuprimeCam, and the Dark Energy Camera. Because these variants serve as testbeds for AP-specific algorithms and configuration settings, they are, as much as possible, the “same” pipeline, differing almost entirely in loading instrument defaults from `obs` packages (§3.2). The only other customization is an extra task for handling DECam’s inter-chip crosstalk, which does not have an equivalent for Rubin instruments.

## 12. CATALOG SCHEMAS

Must transform pipeline products from the internal data model to the public data model defined in M. Jurić et al. (2023).

`sdm_schemas`

`felis` (J. McCormick et al. 2024)

## 13. DISPLAY ABSTRACTIONS

The Python object representing an image with meta-data is a bespoke object not understood by generic tooling. To display an image we provide a display abstraction layer that allows the image to be displayed and graphics overlaid by using a plugin mechanism.

In some plugins the pixel data can be extracted from the exposure object and sent directly to display, in other plugins we form a simple single HDU FITS image (possibly with simplified world coordinates) and pass the temporary FITS file to the display system.

There are currently plugins for matplotlib (J. D. Hunter 2007), Firefly (W. Roby et al. 2020), SAOImage DS9 (W. A. Joye & E. Mandel 2003), and Ginga (E. Jeschke et al. 2013, via Astrowidgets).

## 14. DATA ANALYSIS

`analysis_tools`

`verify`

`faro` — do not document this as we are no longer using it for primary metrics calculation.

## 15. VALIDATING THE SCIENCE PIPELINES

We use small, of order of a few gigabyte, datasets that can be processed as part of continuous integration. These take of order an hour to process. There are regular re-processings of standard datasets that can take a few days to process. For formal data releases there are additional metrics calculated and a test report is issued, such as the one made available with release 28.0 (J. Carlin 2025).

15.1. *Source Injection*

## 16. CONCLUSIONS

The LSST Science Pipelines Software has been developed over 20 years to support the processing of the Legacy Survey of Space and Time.

## ACKNOWLEDGMENTS

This material is based upon work supported in part by the National Science Foundation through Coopera-

tive Agreement AST-1258333 and Cooperative Support Agreement AST-1202910 managed by the Association of Universities for Research in Astronomy (AURA), and the Department of Energy under Contract No. DE-AC02-76SF00515 with the SLAC National Accelerator Laboratory managed by Stanford University. Additional Rubin Observatory funding comes from private donations, grants to universities, and in-kind support from LSSTC Institutional Members.

*Facilities:* Rubin:Simonyi (LSSTCam), Rubin:1.2m (LATISS)

*Software:* ndarray (<https://github.com/ndarray/ndarray>), astropy (Astropy Collaboration et al. 2022), pytest (H. Krekel 2017), matplotlib (J. D. Hunter 2007), galsim (B. T. P. Rowe et al. 2015), numpy (C. R. Harris et al. 2020), gbdes (G. M. Bernstein 2022), Starlink's (D. Berry et al. 2022) AST (D. S. Berry et al. 2016), fgcm (<https://github.com/erykoff/fgcm>),

## REFERENCES

- Alard, C., & Lupton, R. H. 1998, A Method for Optimal Image Subtraction, *ApJ*, 503, 325, doi: [10.1086/305984](https://doi.org/10.1086/305984)
- Astropy Collaboration, Price-Whelan, A. M., Sipőcz, B. M., et al. 2018, The Astropy Project: Building an Open-science Project and Status of the v2.0 Core Package, *AJ*, 156, 123, doi: [10.3847/1538-3881/aabc4f](https://doi.org/10.3847/1538-3881/aabc4f)
- Astropy Collaboration, Price-Whelan, A. M., Lim, P. L., et al. 2022, The Astropy Project: Sustaining and Growing a Community-oriented Open-source Project and the Latest Major Release (v5.0) of the Core Package, *ApJ*, 935, 167, doi: [10.3847/1538-4357/ac7c74](https://doi.org/10.3847/1538-4357/ac7c74)
- Axelrod, T., Connolly, A., Ivezić, Z., et al. 2004, The LSST Data Processing Pipeline, in *American Astronomical Society Meeting Abstracts*, Vol. 205, American Astronomical Society Meeting Abstracts, 108.11
- Axelrod, T., Kantor, J., Lupton, R. H., & Pierfederici, F. 2010, An open source application framework for astronomical imaging pipelines, in *Proc. SPIE*, Vol. 7740, *Software and Cyberinfrastructure for Astronomy*, ed. N. M. Radziwill & A. Bridger, 15, doi: [10.1117/12.857297](https://doi.org/10.1117/12.857297)
- Berk, A., Anderson, G. P., Bernstein, L. S., et al. 1999, MODTRAN4 radiative transfer modeling for atmospheric correction, in *Society of Photo-Optical Instrumentation Engineers (SPIE) Conference Series*, Vol. 3756, *Optical Spectroscopic Techniques and Instrumentation for Atmospheric and Space Research III*, ed. A. M. Larar, International Society for Optics and Photonics (SPIE), 348 – 353, doi: [10.1117/12.366388](https://doi.org/10.1117/12.366388)
- Bernstein, G. M. 2022, gbdes: DECam instrumental signature fitting and processing programs,, *Astrophysics Source Code Library*, record ascl:2210.011
- Bernstein, G. M., Armstrong, R., Plazas, A. A., et al. 2017, Astrometric Calibration and Performance of the Dark Energy Camera, *PASP*, 129, 074503, doi: [10.1088/1538-3873/aa6c55](https://doi.org/10.1088/1538-3873/aa6c55)
- Berry, D., Graves, S., Bell, G. S., et al. 2022, Starlink - The Original and Best, in *Astronomical Society of the Pacific Conference Series*, Vol. 532, *Astronomical Data Analysis Software and Systems XXX*, ed. J. E. Ruiz, F. Pierfederici, & P. Teuben, 559
- Berry, D. S., Warren-Smith, R. F., & Jenness, T. 2016, AST: A library for modelling and manipulating coordinate systems, *Astronomy and Computing*, 15, 33, doi: [10.1016/j.ascom.2016.02.003](https://doi.org/10.1016/j.ascom.2016.02.003)

- Bloom, J. S., Richards, J. W., Nugent, P. E., et al. 2012, Automating Discovery and Classification of Transients and Variable Stars in the Synoptic Survey Era, *PASP*, 124, 1175, doi: [10.1086/668468](https://doi.org/10.1086/668468)
- Bohlin, R. C. 2007, HST Stellar Standards with 1% Accuracy in Absolute Flux, in *Astronomical Society of the Pacific Conference Series*, Vol. 364, *The Future of Photometric, Spectrophotometric and Polarimetric Standardization*, ed. C. Sterken, 315, doi: [10.48550/arXiv.astro-ph/0608715](https://doi.org/10.48550/arXiv.astro-ph/0608715)
- Bosch, J., Armstrong, R., Bickerton, S., et al. 2018, The Hyper Suprime-Cam software pipeline, *PASJ*, 70, S5, doi: [10.1093/pasj/psx080](https://doi.org/10.1093/pasj/psx080)
- Boulade, O., Charlot, X., Abbon, P., et al. 2003, MegaCam: the new Canada-France-Hawaii Telescope wide-field imaging camera, in *Society of Photo-Optical Instrumentation Engineers (SPIE) Conference Series*, Vol. 4841, *Instrument Design and Performance for Optical/Infrared Ground-based Telescopes*, ed. M. Iye & A. F. M. Moorwood, 72–81, doi: [10.1117/12.459890](https://doi.org/10.1117/12.459890)
- Broughton, A., Utsumi, Y., Plazas Malagón, A. A., et al. 2024, Mitigation of the Brighter-fatter Effect in the LSST Camera, *PASP*, 136, 045003, doi: [10.1088/1538-3873/ad3aa2](https://doi.org/10.1088/1538-3873/ad3aa2)
- Burke, D. L., Rykoff, E. S., Allam, S., et al. 2018, Forward Global Photometric Calibration of the Dark Energy Survey, *AJ*, 155, 41, doi: [10.3847/1538-3881/aa9f22](https://doi.org/10.3847/1538-3881/aa9f22)
- Cai, M., Xu, Z., Fan, L., et al. 2025, The 2.5-meter Wide Field Survey Telescope Real-time Data Processing Pipeline I: From raw data to alert distribution, *arXiv e-prints*, *arXiv:2501.15018*, doi: [10.48550/arXiv.2501.15018](https://doi.org/10.48550/arXiv.2501.15018)
- Carlin, J. 2025, Characterization Metric Report: Science Pipelines Version 28.0.0, *Data Management Test Report DMTR-451*, Vera C. Rubin Observatory. <https://dmtr-451.lsst.io/>
- DePoy, D. L., Abbott, T., Annis, J., et al. 2008, The Dark Energy Camera (DECam), in *Society of Photo-Optical Instrumentation Engineers (SPIE) Conference Series*, Vol. 7014, *Ground-based and Airborne Instrumentation for Astronomy II*, ed. I. S. McLean & M. M. Casali, 70140E, doi: [10.1117/12.789466](https://doi.org/10.1117/12.789466)
- Duev, D. A., Mahabal, A., Masci, F. J., et al. 2019, Real-bogus classification for the Zwicky Transient Facility using deep learning, *MNRAS*, 489, 3582, doi: [10.1093/mnras/stz2357](https://doi.org/10.1093/mnras/stz2357)
- Esteves, J. H., Utsumi, Y., Snyder, A., et al. 2023, Photometry, Centroid and Point-spread Function Measurements in the LSST Camera Focal Plane Using Artificial Stars, *PASP*, 135, 115003, doi: [10.1088/1538-3873/ad0a73](https://doi.org/10.1088/1538-3873/ad0a73)
- Fagrelus, P., & Rykoff, E. 2025, Rubin Baseline Calibration Plan, Commissioning Technical Note SITCOMTN-086, Vera C. Rubin Observatory. <https://sitcomtn-086.lsst.io/>
- Fausti, A. 2023, Sasquatch: beyond the EFD, SQuaRE Technical Note SQR-068, Vera C. Rubin Observatory. <https://sqr-068.lsst.io/>
- Fausti Neto, A., Economou, F., Reuter, M. A., et al. 2024, Sasquatch: Rubin Observatory metrics and telemetry service, in *Society of Photo-Optical Instrumentation Engineers (SPIE) Conference Series*, Vol. 13101, *Software and Cyberinfrastructure for Astronomy VIII*, ed. J. Ibsen & G. Chiozzi, 131011M, doi: [10.1117/12.3019081](https://doi.org/10.1117/12.3019081)
- Flaughar, B., Diehl, H. T., Honscheid, K., et al. 2015, The Dark Energy Camera, *The Astronomical Journal*, 150, 150, doi: [10.1088/0004-6256/150/5/150](https://doi.org/10.1088/0004-6256/150/5/150)
- Goldstein, D. A., D’Andrea, C. B., Fischer, J. A., et al. 2015, Automated Transient Identification in the Dark Energy Survey, *AJ*, 150, 82, doi: [10.1088/0004-6256/150/3/82](https://doi.org/10.1088/0004-6256/150/3/82)
- Gower, M., Kowalik, M., Lust, N. B., Bosch, J. F., & Jenness, T. 2022, Adding Workflow Management Flexibility to LSST Pipelines Execution, *arXiv e-prints*, *arXiv:2211.15795*, doi: [10.48550/arXiv.2211.15795](https://doi.org/10.48550/arXiv.2211.15795)
- Harris, C. R., Millman, K. J., van der Walt, S. J., et al. 2020, Array programming with NumPy, *Nature*, 585, 357, doi: [10.1038/s41586-020-2649-2](https://doi.org/10.1038/s41586-020-2649-2)
- Hirata, C., & Seljak, U. 2003, Shear calibration biases in weak-lensing surveys, *MNRAS*, 343, 459, doi: [10.1046/j.1365-8711.2003.06683.x](https://doi.org/10.1046/j.1365-8711.2003.06683.x)
- Hunter, J. D. 2007, Matplotlib: A 2D Graphics Environment, *Computing in Science and Engineering*, 9, 90, doi: [10.1109/MCSE.2007.55](https://doi.org/10.1109/MCSE.2007.55)
- Ingraham, P., Clements, A. W., Ribeiro, T., et al. 2020, Vera C. Rubin Observatory auxiliary telescope commissioning as a control system pathfinder, in *Society of Photo-Optical Instrumentation Engineers (SPIE) Conference Series*, Vol. 11452, *Software and Cyberinfrastructure for Astronomy VI*, ed. J. C. Guzman & J. Ibsen, 114520U, doi: [10.1117/12.2561112](https://doi.org/10.1117/12.2561112)
- Ivezić, Ž., Kahn, S. M., Tyson, J. A., et al. 2019, LSST: From Science Drivers to Reference Design and Anticipated Data Products, *ApJ*, 873, 111, doi: [10.3847/1538-4357/ab042c](https://doi.org/10.3847/1538-4357/ab042c)

- Jarvis, M., Meyers, J., Leget, P.-F., & Davis, C. 2021a, Piff: PSFs In the Full FOV,, Astrophysics Source Code Library, record ascl:2102.024
- Jarvis, M., Bernstein, G. M., Amon, A., et al. 2021b, Dark Energy Survey year 3 results: point spread function modelling, *MNRAS*, 501, 1282, doi: [10.1093/mnras/staa3679](https://doi.org/10.1093/mnras/staa3679)
- Jenness, T. 2020, Modern Python at the Large Synoptic Survey Telescope, in *Astronomical Society of the Pacific Conference Series*, Vol. 522, *Astronomical Data Analysis Software and Systems XXVII*, ed. P. Ballester, J. Ibsen, M. Solar, & K. Shortridge, 541, doi: [10.48550/arXiv.1712.00461](https://doi.org/10.48550/arXiv.1712.00461)
- Jenness, T., Economou, F., Findeisen, K., et al. 2018, LSST data management software development practices and tools, in *Proc. SPIE*, Vol. 10707, *Software and Cyberinfrastructure for Astronomy V*, 1070709, doi: [10.1117/12.2312157](https://doi.org/10.1117/12.2312157)
- Jenness, T., Bosch, J., Owen, R., et al. 2016, Investigating interoperability of the LSST data management software stack with Astropy, in *Proc. SPIE*, Vol. 9913, *Software and Cyberinfrastructure for Astronomy IV*, 99130G, doi: [10.1117/12.2231313](https://doi.org/10.1117/12.2231313)
- Jenness, T., Bosch, J. F., Salnikov, A., et al. 2022, The Vera C. Rubin Observatory Data Butler and pipeline execution system, in *Society of Photo-Optical Instrumentation Engineers (SPIE) Conference Series*, Vol. 12189, *Software and Cyberinfrastructure for Astronomy VII*, 1218911, doi: [10.1117/12.2629569](https://doi.org/10.1117/12.2629569)
- Jeschke, E., Inagaki, T., & Kackley, R. 2013, Introducing the Ginga FITS Viewer and Toolkit, in *Astronomical Society of the Pacific Conference Series*, Vol. 475, *Astronomical Data Analysis Software and Systems XXII*, ed. D. N. Friedel, 319
- Joye, W. A., & Mandel, E. 2003, New Features of SAOImage DS9, in *Astronomical Society of the Pacific Conference Series*, Vol. 295, *Astronomical Data Analysis Software and Systems XII*, ed. H. E. Payne, R. I. Jedrzejewski, & R. N. Hook, 489
- Jurić, M., Ciardi, D., Dubois-Felsmann, G., & Guy, L. 2019, LSST Science Platform Vision Document, Systems Engineering Controlled Document LSE-319, Vera C. Rubin Observatory. <https://lse-319.lsst.io/>
- Jurić, M., Kantor, J., Lim, K. T., et al. 2017, The LSST Data Management System, in *Astronomical Society of the Pacific Conference Series*, Vol. 512, *Astronomical Data Analysis Software and Systems XXV*, ed. N. P. F. Lorente, K. Shortridge, & R. Wayth, 279, doi: [10.48550/arXiv.1512.07914](https://doi.org/10.48550/arXiv.1512.07914)
- Jurić, M., Axelrod, T., Becker, A., et al. 2023, Data Products Definition Document, Systems Engineering Controlled Document LSE-163, Vera C. Rubin Observatory. <https://lse-163.lsst.io/>
- Kahn, S. M., Kurita, N., Gilmore, K., et al. 2010, Design and development of the 3.2 gigapixel camera for the Large Synoptic Survey Telescope, in *Society of Photo-Optical Instrumentation Engineers (SPIE) Conference Series*, Vol. 7735, *Ground-based and Airborne Instrumentation for Astronomy III*, ed. I. S. McLean, S. K. Ramsay, & H. Takami, 0, doi: [10.1117/12.857920](https://doi.org/10.1117/12.857920)
- Kannawadi, A. 2022, Consistent galaxy colors with Gaussian-Aperture and PSF photometry, Data Management Technical Note DMTN-190, Vera C. Rubin Observatory. <https://dmtn-190.lsst.io/>
- Karavakis, E., Guan, W., Yang, Z., et al. 2024, Integrating the PanDA Workload Management System with the Vera C. Rubin Observatory, in *European Physical Journal Web of Conferences*, Vol. 295, *European Physical Journal Web of Conferences (EDP)*, 04026, doi: [10.1051/epjconf/202429504026](https://doi.org/10.1051/epjconf/202429504026)
- Knight, S. 2005, Building software with SCons, *Computing in Science Engineering*, 7, 79, doi: [10.1109/MCSE.2005.11](https://doi.org/10.1109/MCSE.2005.11)
- Krekel, H. 2017, pytest: helps you write better programs, <https://docs.pytest.org>
- Kuijken, K. 2008, GaaP: PSF- and aperture-matched photometry using shapelets, *A&A*, 482, 1053, doi: [10.1051/0004-6361:20066601](https://doi.org/10.1051/0004-6361:20066601)
- Kuijken, K., Heymans, C., Hildebrandt, H., et al. 2015, Gravitational lensing analysis of the Kilo-Degree Survey, *MNRAS*, 454, 3500, doi: [10.1093/mnras/stv2140](https://doi.org/10.1093/mnras/stv2140)
- Lange, T., Nordby, M., Pollek, H., et al. 2024, Integrating the LSST camera, in *Society of Photo-Optical Instrumentation Engineers (SPIE) Conference Series*, Vol. 13096, *Ground-based and Airborne Instrumentation for Astronomy X*, ed. J. J. Bryant, K. Motohara, & J. R. D. Vernet, 130961O, doi: [10.1117/12.3019302](https://doi.org/10.1117/12.3019302)
- Li, X., Miyatake, H., Luo, W., et al. 2022, The three-year shear catalog of the Subaru Hyper Suprime-Cam SSP Survey, *PASJ*, 74, 421, doi: [10.1093/pasj/psac006](https://doi.org/10.1093/pasj/psac006)
- Lim, K.-T. 2022, Proposal and Prototype for Prompt Processing, Data Management Technical Note DMTN-219, Vera C. Rubin Observatory. <https://dmtn-219.lsst.io/>
- Lupton, R., Malagón, A. A. P., & Waters, C. 2025, Verifying LSST Calibration Data Products, Data Management Technical Note DMTN-101, Vera C. Rubin Observatory. <https://dmtn-101.lsst.io/>



- Lust, N. B., Jenness, T., Bosch, J. F., et al. 2023, Data management and execution systems for the Rubin Observatory Science Pipelines, arXiv e-prints, arXiv:2303.03313, doi: [10.48550/arXiv.2303.03313](https://doi.org/10.48550/arXiv.2303.03313)
- Mandelbaum, R., Hirata, C. M., Seljak, U., et al. 2005, Systematic errors in weak lensing: application to SDSS galaxy-galaxy weak lensing, MNRAS, 361, 1287, doi: [10.1111/j.1365-2966.2005.09282.x](https://doi.org/10.1111/j.1365-2966.2005.09282.x)
- Mandelbaum, R., Miyatake, H., Hamana, T., et al. 2018, The first-year shear catalog of the Subaru Hyper Suprime-Cam Subaru Strategic Program Survey, PASJ, 70, S25, doi: [10.1093/pasj/psx130](https://doi.org/10.1093/pasj/psx130)
- McCormick, J., Dubois-Felsmann, G. P., Salnikov, A., Van Klaveren, B., & Jenness, T. 2024, Using Felis to Represent the Semantics and Metadata of Astronomical Data Catalogs, arXiv e-prints, arXiv:2412.09721, doi: [10.48550/arXiv.2412.09721](https://doi.org/10.48550/arXiv.2412.09721)
- Miyazaki, S., Komiyama, Y., Kawanomoto, S., et al. 2018, Hyper Suprime-Cam: System design and verification of image quality, PASJ, 70, S1, doi: [10.1093/pasj/psx063](https://doi.org/10.1093/pasj/psx063)
- Morrison, C. B. 2018, Pessimistic Pattern Matching for LSST, Data Management Technical Note DMTN-031, Vera C. Rubin Observatory. <https://dmtn-031.lsst.io/>
- Mueller, F., et al. 2023, Qserv: A Distributed Petascale Database for the LSST Catalogs, in ASP Conf. Ser., Vol. TBD, ADASS XXXII, ed. S. Gaudet, S. Gwyn, P. Dowler, D. Bohlender, & A. Hincks (San Francisco: ASP), in press. <https://dmtn-243.lsst.io>
- Mullaney, J. R., Makrygianni, L., Dhillon, V., et al. 2021, Processing GOTO data with the Rubin Observatory LSST Science Pipelines I: Production of coadded frames, PASA, 38, e004, doi: [10.1017/pasa.2020.45](https://doi.org/10.1017/pasa.2020.45)
- Okura, Y., Petri, A., May, M., Plazas, A. A., & Tamagawa, T. 2016, Consequences of CCD Imperfections for Cosmology Determined by Weak Lensing Surveys: From Laboratory Measurements to Cosmological Parameter Bias, The Astrophysical Journal, 825, 61, doi: [10.3847/0004-637X/825/1/61](https://doi.org/10.3847/0004-637X/825/1/61)
- Okura, Y., Plazas, A. A., May, M., & Tamagawa, T. 2015, Spurious shear induced by the tree rings of the LSST CCDs, Journal of Instrumentation, 10, C08010, doi: [10.1088/1748-0221/10/08/C08010](https://doi.org/10.1088/1748-0221/10/08/C08010)
- O'Mullane, W., Economou, F., Lim, K.-T., et al. 2022, Software Architecture and System Design of Rubin Observatory, arXiv e-prints, arXiv:2211.13611, doi: [10.48550/arXiv.2211.13611](https://doi.org/10.48550/arXiv.2211.13611)
- O'Mullane, W., Economou, F., Huang, F., et al. 2024, Rubin Science Platform on Google: the story so far, in Astronomical Society of the Pacific Conference Series, Vol. 535, Astromical Data Analysis Software and Systems XXXI, ed. B. V. Hugo, R. Van Rooyen, & O. M. Smirnov, 227, doi: [10.48550/arXiv.2111.15030](https://doi.org/10.48550/arXiv.2111.15030)
- O'Mullane, W., Allbery, R., AlSayyad, Y., et al. 2024, Rubin Observatory Data Security Standards Implementation, Data Management Technical Note DMTN-199, Vera C. Rubin Observatory. <https://dmtn-199.lsst.io/>
- Padmanabhan, N., Lupton, R., & Loomis, C. 2015, EUPS — a Tool to Manage Software Dependencies, <https://github.com/RobertLuptonTheGood/eups>
- Park, H., Karpov, S., Nomerotski, A., & Tsybychev, D. 2020, Tree rings in Large Synoptic Survey Telescope production sensors: its dependence on radius, wavelength, and back bias voltage, Journal of Astronomical Telescopes, Instruments, and Systems, 6, 011005, doi: [10.1117/1.JATIS.6.1.011005](https://doi.org/10.1117/1.JATIS.6.1.011005)
- Park, H. Y., Nomerotski, A., & Tsybychev, D. 2017, Properties of tree rings in LSST sensors, Journal of Instrumentation, 12, C05015, doi: [10.1088/1748-0221/12/05/C05015](https://doi.org/10.1088/1748-0221/12/05/C05015)
- Paszke, A., Gross, S., Massa, F., et al. 2019, PyTorch: An Imperative Style, High-Performance Deep Learning Library, in Advances in Neural Information Processing Systems, ed. H. Wallach, H. Larochelle, A. Beygelzimer, F. d'Alché-Buc, E. Fox, & R. Garnett, Vol. 32 (Curran Associates, Inc.), doi: [10.48550/arXiv.1912.01703](https://doi.org/10.48550/arXiv.1912.01703)
- Patterson, M., Bellm, E., Swinbank, J., & Nelson, S. 2020, Design of the LSST Alert Distribution System, Data Management Technical Note DMTN-093, Vera C. Rubin Observatory. <https://dmtn-093.lsst.io/>
- Pier, J. R., Munn, J. A., Hindsley, R. B., et al. 2003, Astrometric Calibration of the Sloan Digital Sky Survey, AJ, 125, 1559, doi: [10.1086/346138](https://doi.org/10.1086/346138)
- Plazas Malagón, A. A., Waters, C., Broughton, A., et al. 2024, Instrument Signature Removal and Calibration Products for the Rubin Legacy Survey of Space and Time, arXiv e-prints, arXiv:2404.14516, doi: [10.48550/arXiv.2404.14516](https://doi.org/10.48550/arXiv.2404.14516)
- Reiss, D. J., & Lupton, R. H. 2016, Implementation of Image Difference Decorrelation, Data Management Technical Note DMTN-021, Vera C. Rubin Observatory. <https://dmtn-021.lsst.io/>



- Roby, W., Wu, X., Dubois-Felmann, G., et al. 2020, Firefly and Python — New Ways to Visualize Data on the Web, in *Astronomical Society of the Pacific Conference Series*, Vol. 527, *Astronomical Data Analysis Software and Systems XXIX*, ed. R. Pizzo, E. R. Deul, J. D. Mol, J. de Plaa, & H. Verhouwer, 243
- Roodman, A., Rasmussen, A., Bradshaw, A., et al. 2024, LSST camera verification testing and characterization, in *Ground-based and Airborne Instrumentation for Astronomy X*, ed. J. J. Bryant, K. Motohara, & J. R. D. Vernet, Vol. 13096, *International Society for Optics and Photonics (SPIE)*, 130961S, doi: [10.1117/12.3019698](https://doi.org/10.1117/12.3019698)
- Rowe, B. T. P., Jarvis, M., Mandelbaum, R., et al. 2015, GALSIM: The modular galaxy image simulation toolkit, *Astronomy and Computing*, 10, 121, doi: [10.1016/j.ascom.2015.02.002](https://doi.org/10.1016/j.ascom.2015.02.002)
- Salnikov, A., & McCormick, J. 2024, Current status of APDB and PPDB implementation, *Data Management Technical Note DMTN-293*, Vera C. Rubin Observatory. <https://dmtn-293.lsst.io/>
- Schutt, T., Jarvis, M., Roodman, A., et al. 2025, Dark Energy Survey Year 6 Results: Point-Spread Function Modeling, *The Open Journal of Astrophysics*, 8, 26, doi: [10.33232/001c.132299](https://doi.org/10.33232/001c.132299)
- Sutherland, W., Emerson, J., Dalton, G., et al. 2015, The Visible and Infrared Survey Telescope for Astronomy (VISTA): Design, technical overview, and performance, *A&A*, 575, A25, doi: [10.1051/0004-6361/201424973](https://doi.org/10.1051/0004-6361/201424973)
- Thomas, S. J., Barr, J., Callahan, S., et al. 2022, Rubin Observatory Simonyi Survey Telescope status overview, in *Society of Photo-Optical Instrumentation Engineers (SPIE) Conference Series*, Vol. 12182, *Ground-based and Airborne Telescopes IX*, ed. H. K. Marshall, J. Spyromilio, & T. Usuda, 121820W, doi: [10.1117/12.2630226](https://doi.org/10.1117/12.2630226)
- Utsumi, Y., Antilogus, P., Astier, P., et al. 2024, LSST Camera focal plane optimization, in *X-Ray, Optical, and Infrared Detectors for Astronomy XI*, ed. A. D. Holland & K. Minoglou, Vol. 13103, *International Society for Optics and Photonics (SPIE)*, 131030W, doi: [10.1117/12.3019117](https://doi.org/10.1117/12.3019117)
- van Rossum, G. 2013, PEP 8 – Style Guide for Python Code, Python Software Foundation. <https://www.python.org/dev/peps/pep-0008/>
- Wang, D. L., Monkewitz, S. M., Lim, K.-T., & Becla, J. 2011, Qserv: A Distributed Shared-nothing Database for the LSST Catalog, in *State of the Practice Reports, SC '11* (New York, NY, USA: ACM), 12:1–12:11, doi: [10.1145/2063348.2063364](https://doi.org/10.1145/2063348.2063364)
- Wang, S.-Y., Huang, P.-J., Chen, H.-Y., et al. 2020, Prime Focus Spectrograph (PFS): the prime focus instrument, in *Society of Photo-Optical Instrumentation Engineers (SPIE) Conference Series*, Vol. 11447, *Ground-based and Airborne Instrumentation for Astronomy VIII*, ed. C. J. Evans, J. J. Bryant, & K. Motohara, 114477V, doi: [10.1117/12.2561194](https://doi.org/10.1117/12.2561194)
- Waters, C. 2025, Calibration Generation, Verification, Acceptance, and Certification., *Data Management Technical Note DMTN-222*, Vera C. Rubin Observatory. <https://dmtn-222.lsst.io/>
- Waters, C. Z., Magnier, E. A., Price, P. A., et al. 2020, Pan-STARRS Pixel Processing: Detrending, Warping, Stacking, *ApJS*, 251, 4, doi: [10.3847/1538-4365/abb82b](https://doi.org/10.3847/1538-4365/abb82b)
- Wright, A. H., Kuijken, K., Hildebrandt, H., et al. 2025, The fifth data release of the Kilo Degree Survey: Multi-epoch optical/NIR imaging covering wide and legacy-calibration fields, *arXiv e-prints*, arXiv:2503.19439. <https://arxiv.org/abs/2503.19439>
- Zackay, B., Ofek, E. O., & Gal-Yam, A. 2016, Proper Image Subtraction—Optimal Transient Detection, Photometry, and Hypothesis Testing, *ApJ*, 830, 27, doi: [10.3847/0004-637X/830/1/27](https://doi.org/10.3847/0004-637X/830/1/27)